International Review of Electrical Engineering (I.R.E.E.), Vol. 9, N. 5
ISSN 1827- 6660 pp.1049-1059 September – October 2014

Novel Approach of Arcing Faults Electromagnetic Radiated Energy Source Location Using Antennas in Power Systems

Frank Zoko Ble, Matti Lehtonen, Charles Kim

Abstract – *This paper presents novel approach of power arcing faults source location using the arc electromagnetic (EM) radiated energy absorbed by strategically placed antennas. Real electric arc was reproduced during a laboratory measurement by a pine tree leaned on an energized current conductor to mimic actual arcing fault phenomenon. Once the arc RF signal data were gathered, only the first cycle of the arrival wave front was considered in order to minimize the effect of the signal reflections from the walls of the measurement room. Using the signal energy contained in this first cycle the Inverse Square Law (ISL) was exploited to derive the distance that separates the antennas from the arcing fault source point. Subsequently the Arc Source Cartesian Coordinates (ASCC) were calculated via iteration method. Next the measured and actual ASCC were compared and the results show that this new approach of using exclusively the arc EM radiated energy can be integrated in power systems as an arcing faults monitoring device to supplement the conventional fault detection methods.*

***Keywords**: Power Arc, Radio Frequency, Electromagnetic Radiation, Antenna, Signal Arrival Time, Arc Source Location, Signal Processing, Radio Signal Propagation, Time Delay Estimation, Radio Measurement*

Nomenclature

DF	Directional Finding
PA	Propagation Attenuation
RF	Radio Frequency
TDOA	Time Difference of Arrival
DDOA	Distance Difference of Arrival
DOA	Distance of Arrival
TOA	Time of Arrival
ASCC	Arc Source Cartesian Coordinates
ISL	Inverse Square Law
LSM	Least Square Method
DMS	Distribution Management System
OMS	Outage Management System
FPA	First Peak of Arrival
CB	Circuit breaker
$i_a(t)$	Instantaneous arc current
V_m	Maximum voltage amplitude
R_a	Arc resistance
ω	Angular frequency per cycle
c	Speed of signal wave
$s(t)$	RF-Signal
τ	Time delay
$F(X)$	Non-linear vector function
$X(x_i, y_i, z_i)$	Vector variable
ant_i	Antenna *i*
θ	Angle between voltage and current
DoA	Direction of Arrival
ATD	Arrival Time Difference
AoA	Angle of Arrival
LOS	Line of Sight
GPS	Global Positioning System
HF	High Frequency
VHF	Very High Frequency
VLF	Very Low Frequency
UHF	Ultra High Frequency
V_r	Arc restrike voltage
V_a	Voltage across an arc
L	Arc inductance
N_s	Total number of samples
ρ_{P_T}	Power density
d	Distance
P_R	Power received
P_T	Power transmitted
α	Signal amplitude attenuation factor
A	Signal propagation attenuation
g	Arc conductance
γ	Arc luminance factor
u_a	Arc voltage
U_c	Constant supply voltage
p_a	Arc power
ε_0	Permittivity of air
$E_r(\vec{u}, t)$	Arc radiated energy
$\frac{\partial i}{\partial t}$	Current partial derivative
$ln(.) = log_e(.)$	Natural logarithm
ν	Wave propagation speed
δi	Current variation
μ_0	Absolute permeability of the air

β	Wave propagation angle
E_d	Radial energy unit vector
E_z	Energy unit vector along z-axis
E_ψ	Tangential energy unit vector at ψ
E_φ	Tangential energy unit vector at φ
σ	Signal attenuation factor
f	Wave frequency
i_m	Transient peak current
$\vec{u}$	Distance unit vector
ψ, φ	Angles
Ω	Ohm (impedance unit)

I. Introduction

This paper develops new approach of power arcing fault detection and location, only based on radio frequency (RF) signals energy associated with arcing faults in power systems network. Using strategically placed directional founding sensors such as Yagi-Uda antennas the arc EM signals are recorded and analysed [1]-[3].

Several reviews have shown that the prevailing types of the power arcing faults in power systems network are basically single phase to ground faults [1]- [3].

The detection and location of power arcs is critical for the distribution management system (DMS) and/or outage Management system (OMS) because an accurate location of the fault arcs could minimize power supply restoration outage times under real field conditions. However since the advent of radar system, detecting the electromagnetic radiations sources has become quite prominent and suitable technique for several researchers [1]-[51].

The information extracted via EM radiated signals using four strategically placed directional antennas can be used to pin arc source point position.

As suggested by several existing reviews done by [1] and [3]-[51] the detection and location via power arc EM radiations can be achieved using several techniques like: (i) Angle of RF signal Arrival method (AoA), (ii) RF signal Time difference of Arrival (TDOA) method and (iii) RF signal Propagation Attenuation (PA) method to cite only few. The later method is mainly used in this present paper. Basically dealing with RF signal is not that simple because the interferences related to free space RF noise can affect the integrity of the signal of interest.

But in order to minimize the undesirable effect of the space noise, this paper proposes the use of only the first cycle of the EM wavefront which contains the signal First Peak of Arrival (FPA). Then the corresponding energy can be exploited in conjunction with Inverse Square Law (ISL) to pin arc source point position. The advantage of this new approach is such that prior knowledge of the arc transmitted energy is not necessary.

This paper is organised as follows: Section II presents the power arcing faults conventional-, the arc interruption via circuit breaker- and the arc electromagnetic radiation-models. The experiment designed to detect and locate the power arcing faults together with the experimental results and discussion related to the practical feasibility and limitations of the proposed method are presented in Section III. Finally, in Section IV, the conclusions are given with suggested improvements.

II. Power Arcing Faults

II.1. Power Systems Arcing Fault Conventional Model

Power arcing faults occur usually as an electrical breakdown of a gas which produces persistent plasma discharge in the surrounding region centred at the emission point. Once an arc is ignited its associated electromagnetic field induces a current in an ordinarily nonconductive media like air and the arc discharges phenomenon and mechanism are associated with low current amplitude and high temperature at first stage and current increases rapidly after few microseconds.

This arc high temperature ionises the air or gas molecules to produce additional electrons which sustain and help the arc in burning stage. The study conducted by [3] indicates that the maximum current through an arc is controlled exclusively by the external circuit which does not actually depend on the arc. Such behaviour result in a decrease of arcing fault voltage (V_a) and simultaneously causes the arc current (i_a) to rise rapidly, therefore the arc resistance (R_a) will obviously have a negative slope. The arc current can be modelled as follows:

$$i_a(t) = \int_{t_0}^{t} (V_m\, cos(\omega t + \theta) - V_a) dt \tag{1}$$

where $t_0 = \frac{1}{2\pi f} sin^{-1}\left(\frac{V_r}{V_m}\right)$, $i_a(t)$ is the time dependent arc current, the angular frequency per cycle $\omega = 2\pi f$ (f is a wave frequency), t is the sampling period, V_a is the arc voltage, while V_r and V_m are respectively the arc re-strike and maximum voltages.

However an investigation conducted by [3] showed that in reality the arc has both an inductance and conductance. Therefore the time dependency of such arc current characteristic due to its small inductance and conductance can be modelled using the arc current and its time derivative as expressed in (2) and (3):

$$V_m\, cos(2\pi f t) = i_a R_a + L\frac{di_a}{dt} + V_a \tag{2}$$

$$V_m\, sin(2\pi f t) = i_a R + L\frac{di_a}{dt} + (20 + 534g) i_a^{\gamma} \tag{3}$$

where L and g are respectively the arc inductance and conductance and the constant γ is the arc luminance factor which exclusively depends on the arc propagation medium (i.e. air in this paper), the arc voltage and current.

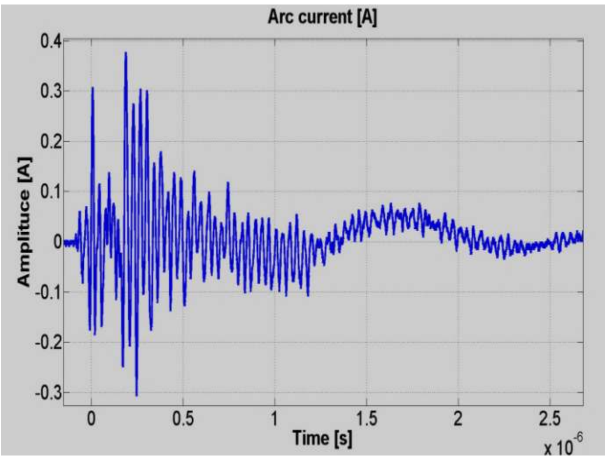

Fig. 1. Recorded arc current

II.2. Circuit Breaker Interruption Models

Under both normal and abnormal field conditions circuit breakers (CB) are usually used to interrupt the load supply in power systems network.

These interruptions are done when CB is suddenly opened, giving rise to an arc ignition. In order to study these arcs due to CB, Mayr and Cassie have developed two models which establish a relation between the arc conductance with arc voltage and power. The formulations of these models are respectively as follows: (4) for Mayr arc model and (5) for Cassie arc representation ([3] and [52]):

$$\frac{1}{g}\frac{dg}{dt} = \frac{d\ln(g)}{dt} = \frac{1}{\tau}\left(\frac{u_a . i_a}{p_a} - 1\right) \tag{4}$$

$$\frac{1}{g}\frac{dg}{dt} = \frac{d\ln(g)}{dt} = \frac{1}{\tau}\left(\frac{{u_a}^2}{U_c} - 1\right) \tag{5}$$

where i_a is the arc current, u_a the arc voltage, p_a the arc cooling power, g the arc conductance, τ the arc time constant, U_c the constant supply voltage and $ln(.) = log_e(.)$ the natural logarithm where $e \approx 2.718$.

The next section will examine the energy radiation mathematical theory and its feasibility in arc fault detection and location.

II.3. Electromagnetic Energy Radiation Model

RF signals can travel from the EM radiated source point to the receiver (namely antenna) by propagating in free space or via a medium. Assume power arc fault as dipole source such as illustrated in Figure 2 and if the arc source EM energy is radiated uniformly in all directions, then it is said to be isotropic and energy propagates outward spherically. [1]

Then any directional finding antenna placed at a distance (d) from that EM source point will be enclosed in the sphere of radius (d) and the antenna receives an energy expressed as [3]:

$$E_r(\vec{u}, t) = \frac{sin(\psi)}{4\pi\varepsilon_0 dc^2}\int_0^M \left(\frac{di}{dt}\right) dt \tag{6}$$

where $E_r(d,t)$ is the arc radiated energy which is function of both distance (d) and time (t), ψ is the phase angle between the current direction and the distance unit vector $\vec{\boldsymbol{u}} = \vec{\boldsymbol{d}}/\|\vec{\boldsymbol{d}}\|$, ε_0 is the permittivity of air, c is the speed of light and M is the total length of the current (i).

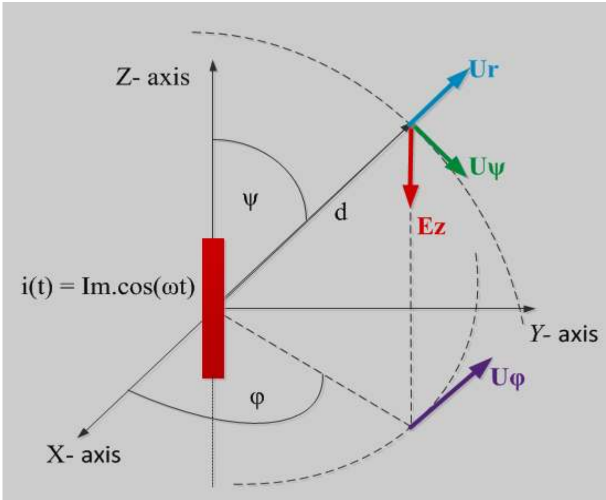

Fig. 2. Arc current representation

Taking a time derivative of the arc current as shown in (7) gives the arc associated electric field as illustrated in (8) under the steady state conditions [3]:

$$\frac{di}{dt} = \frac{\partial i}{\partial t} + \frac{\partial i}{\partial z}\frac{\partial z}{\partial t} \tag{7}$$

where $\frac{\partial i}{\partial t}$ and $\frac{\partial i}{\partial z}$ are the partial derivatives of the current respectively in time domain and along the z-direction.

The partial derivative $\frac{\partial z}{\partial t}$ is actually the speed at which the arc current propagates in the z direction [3]:

$$E_r(\vec{u}, t) = \frac{sin(\psi)}{4\pi\varepsilon_0 dc^2}\int_0^L \left(\frac{\partial i}{\partial z}\frac{\partial z}{\partial t}\right) dz \tag{8}$$

The solution of the integral in (8), illustrates a small variation in arc current $\delta i = i_m - i_0$, (where i_m and i_0 are respectively the breakdown transient peak and initial currents [3]:

$$E_r(\vec{u}, t) = \frac{\sin(\psi)}{4\pi\varepsilon_0 dc^2}\nu\delta i \tag{9}$$

where $\nu = \frac{1}{\sqrt{\mu_0\varepsilon_0}}$ is the steady state propagation speed which is assumed to be the speed of light in free space.

Referring to Fig. 2 and assuming a spherical coordinate system frame of reference together with the arc signal angle of arrival which are independent variables $\{\psi,\ d,\ \varphi\}$ the resulting phasor of the potential vector E is given as:

$$E(d) = E_z = \left[\frac{\mu}{4\pi}\right] M \frac{I_m}{d} e^{-j\beta d} \quad , \ \beta = \frac{\omega}{v} \tag{10}$$

$$E_d = E_z \cos\psi \tag{11}$$

$$E_\psi = -E_z \sin(\psi) \tag{12}$$

$$E_\varphi = 0 \tag{13}$$

where $E(d)$ is the arc electric field at distance (d), E_d is the arc radial component in the direction of $\vec{\boldsymbol{U}}_r$, E_ψ is the arc tangential component in the direction of unit vector $\vec{\boldsymbol{U}}_\psi$, E_φ is the arc tangential component in the direction of unit vector $\vec{\boldsymbol{U}}_\varphi$ and $\beta = \frac{\omega}{v}$ is the angle of the signal propagation.

If the arc is located at any point different from the system origin, its 3D coordinates can be calculated when the values of the signal angle of arrival (ϑ_i), (φ_i) and the distance (d_i) that separates antenna i and the arc source for each placement are known, and with an assumption that the antenna i is located on the periphery of the sphere having a radius (d):

$$\boldsymbol{X}_i - \boldsymbol{X}_s = \begin{bmatrix} d_i \cos(\psi_i)\sin(\varphi_i) \\ d_i \sin(\psi_i)\sin(\varphi_i) \\ d_i \cos(\varphi_i) \end{bmatrix} \tag{14}$$

where $\boldsymbol{X}_s = [x_s \quad y_s \quad z_s]^T$ and $\boldsymbol{X}_i = [x_i \quad y_i \quad z_i]^T$ are respectively arc source and antenna i position vectors.

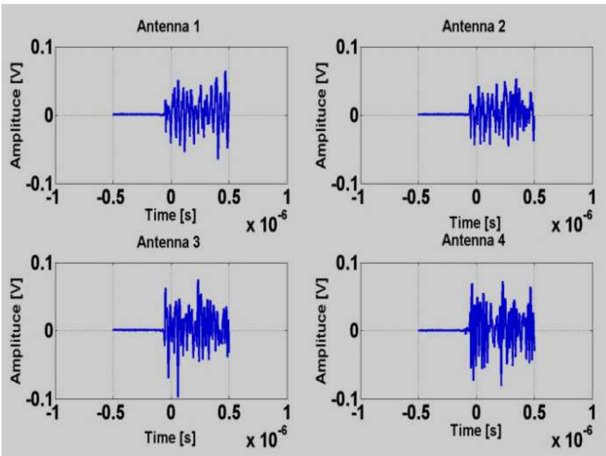

Fig. 3. Recorded arc RF-signals captured by the antennas

After this brief introduction of the electromagnetic energy radiation in free space, its practical application in fault detection and location is discussed in the next section.

II.4. Detection and Location Methods

The electromagnetic radiation can originate from different sources in power system when arcing fault occurs. These arc fault events are caused by: (i) lightning, (ii) switching surges, (iii) trees growing in the vicinity of the load line, (iv) wind causing adjacent conductor touching, (v) wind driven objects, (vi) broken and damaged insulation material and (vii) ice inducing conductor sagging and breaking. Using strategically placed antennas the electromagnetic radiation emitted by arcs can be detected and located according to [1]-[5], [8]-[9], [14], [26], [28], [29], [32], [34], [40], [45].

Once the electromagnetic radiation signal emitted by the arc has been gathered, the recorded data can be analysed using (15) to extract the energy absorbed by the antennas during signal wave front first cycle of arrival.

As seen in (15) $E(t)$ is the total energy captured by the antennas which is obtained by the summation of the squared sample data over the first peak wave front propagation period (T), where $s(t)$ is the signal of interest. Additionally the equation (15) is shown in both continuous time and discrete domains, where N is the total number of samples and $k = 1, 2, 3, \dots N-1$:

$$E(t) = \frac{1}{T}\int_{-T}^{+T} s(t)^2 dt = \frac{1}{N}\sum_{1}^{N-1} s(k)^2 \tag{15}$$

The electromagnetic radiated energy $E(t)$ is scattered as summarized in Table I and plotted as illustrated in Fig. 4 based on antennas' placement 1.

In this experiment 5 antennas' placements as discussed in [1]-[2] are used, and the entire energy results derived from (15) when applied to the real experimental data are shown in Table I.

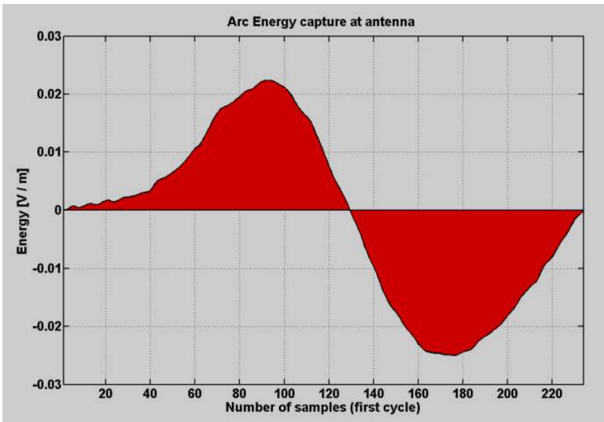

Fig. 4. RF-signal energy in placement 1 of measurement 1

TABLE I
ENERGY [V/M]

Placement	ant1	ant2	ant3	ant4
1	0.000006	0.000013	0.000048	0.000020
2	0.000017	0.000079	0.000209	0.000072
3	0.000013	0.000040	0.000072	0.000117
4	0.000044	0.000141	0.000097	0.000101
5	0.000029	0.000036	0.000032	0.000016

As seen in Table I the absorbed energy varies with respect to the antennas' placement. Referring to Fig. 5 these energy values are distributed as follows: in placement 1 as the 4 antennas are horizontally aligned and the captured energy by antenna 1 is 6% of the total transmitted energy by the arc, while those detected by antennas 2, 3 and 4 are respectively 15%, 56% and 23%.

Similar analogy is all observed for the other placements (see Figs. 13 – 16).

These variations of energy are as expected since antenna 3 is much closer to the source point, and followed respectively by antennas 4, 2 and 1. This follows the signal propagation power density law, Inverse Square Law (ISL) expressed as:

$$E_r \propto \frac{I}{4\pi d^2} \quad (16)$$

where E_r is the received energy, d is the distance between the arc source and the antenna and I is the energy transmitted by the arc source point. The equation (16) implies that in free space, all electromagnetic waves obey the inverse-square law, and the radiated energy emission is proportional to the inverse of the square of the distance from a point source. Fig. 6 shows the absorbed energy by the 4 antennas for each placement.

The experiment setup of the proposed method for arc detection and location is discussed in the next section.

III. Arc Location Experiment and Data Analysis

In order to evaluate the performance of the proposed method, we performed a set of arc location experiments as shown in Figs. 7-8 [1].

III.1. Experiment Set-up

The set-up depicted in Figures 7-8 is similar to the set-up made and discussed in [1]-[2]. It consists of four strategically placed antennas around the arc source covering a portion of RF radiation space. These 4 antennas detect the electromagnetic radiation energy emitted by the arc source formed by a tree leaned on an energized conductor. As mentioned before 5 different antennas' placements were used.

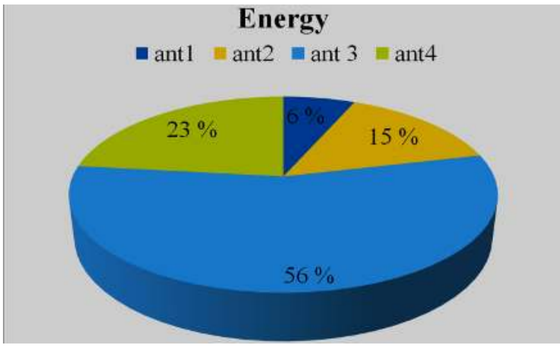

Fig. 5. Energy comparison in placement 1

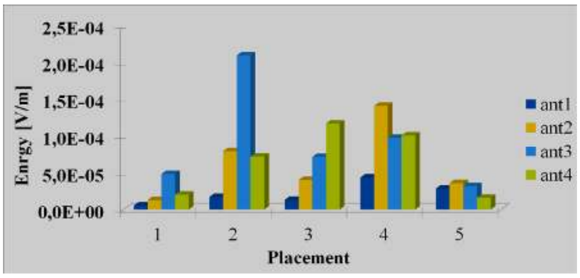

Fig. 6. RF signal energy for the 5 antennas' placements

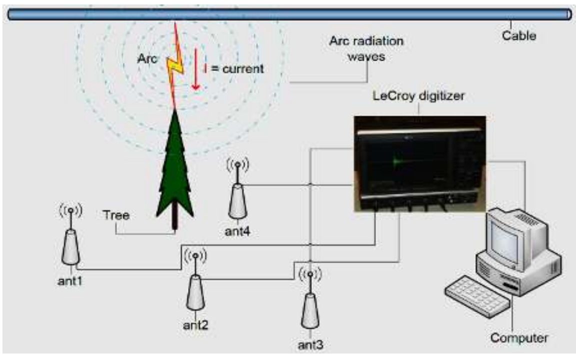

Fig. 7. The experimental setup for arc generation [1]-[2]

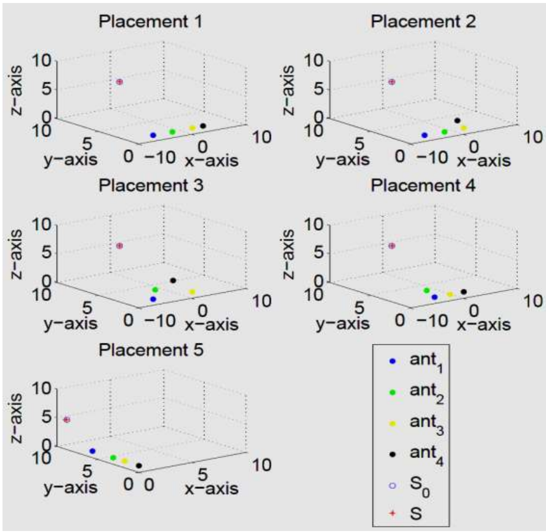

Fig. 8. Antennas placements [1] -[2]

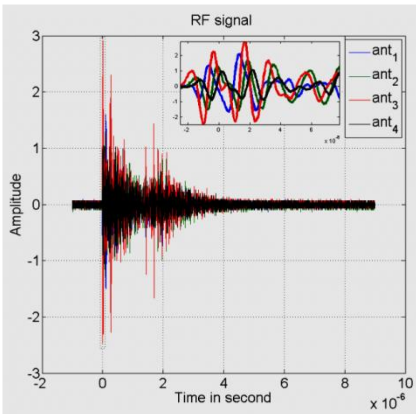

Fig. 9. The captured arc RF signal in placement 1 [1]-[2]

III.2. Results and Discussion

In order to demonstrate the applicability of the proposed arc detection and location method, real data of an experimental mimic power arc electromagnetic radiation was obtained based on strategically placed antennas. These antennas were located at a distance of 2 to 12 m from the source point, in order to detect the radiation emitted by a power arc produced by a pine tree leaned on an energized conductor.

The duration of recording was 1 μs with a sampling ratio of 2×10^9 samples/s and 20002 samples were made available. The arc EM signals obtained in this experiment are shown in Figs. 3 and 9. Based on these figures, two interesting facts emerge as follows: (i) the signals patterns are quite similar showing a suitable scheme using antennas to detect power arc effectively in this proposed method. Next (ii) the relation of the distance between the antennas and the arc source point and the arc signal arrival amplitude shows nonlinear characteristics.

Based on these two aspects, the gathered arc signal radiation energy and the distance define a clear relation which is observable in Fig. 10.

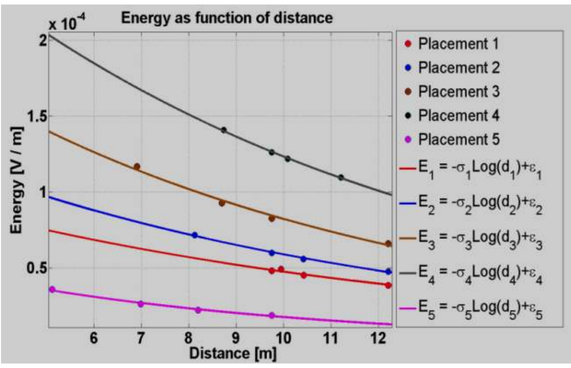

Fig. 10. RF signal energy as function of distance

The antennas' captured signals data were truncated using window techniques in order to extract the First Peak of Arrival (FPA) first cycle.

Then the Eq. (15) was used to calculate the area under the curve as illustrated in Fig. 4 in order to obtain the signal FPA energy and the results are summarized in Table I. Using the actual distance (d) (namely DOA) between the antennas and the power arc source as shown in Table V in conjunction with the calculated energy in Table I, a curve fitting energy-distance equation was formed as (17) and shown in Fig. 10:

$$E\,(d_i) = \sigma_j\, log(d_i) + \varepsilon_j \qquad (17)$$

where σ_j and ε_j are parameter values as summarized in Table II and $j = 1,2, \ldots .5$ is the number of placements. These values are dependent on the antennas placement and varying almost identically as mentioned above.

Assuming that the transmitted radiated energy emitted by the source per placement is constant for the 4 antennas within the same placement, the measured distances between the arc source and the antennas are calculated using (16) and presented in Table IX. The distance (d) and time (t) as discussed in [1]-[2] are proportional since $d = c * t$, where c is the speed of light. Next the signal times of arrival (TOA) are calculated for both actual and measured distances as summarized respectively in Tables III and VII.

From the TOA calculated results, the TDOA are simply obtained using an arithmetic subtraction between pairs of TOA and the outcomes are illustrated respectively for both actual and measured results in Tables VI and VIII. Having obtained the TDOA, the algorithm used to derive the exact arc source point location based on the captured signal data is explained in detail in [1]-[2].

TABLE II
PARAMETERS

Placement	σ_j	ε_j
1	-0.00005	0.0002
2	-0.00006	0.0002
3	-0.00009	0.0003
4	-0.0001	0.0004
5	-0.00003	0.00008

TABLE III
ACTUAL TIME OF ARRIVAL TOA [NS]

Placement	t1	t2	t3	t4
1	40.716	34.745	32.495	33.165
2	40.712	34.742	32.495	27.095
3	40.710	29.002	32.495	23.007
4	37.371	29.116	33.637	32.495
5	17.033	23.293	27.309	32.495

TABLE IV
ACTUAL TIME DIFFERENCE OF ARRIVAL BETWEEN THE ANTENNAS (TDOA) [ns]

Placement	t12	t13	t14	t23	t24	t34
1	5.963	8.201	7.524	2.238	1.561	0.677
2	5.963	8.201	13.594	2.238	7.632	5.393
3	11.704	8.201	17.682	3.503	5.978	9.481
4	8.254	3.728	4.864	4.525	3.389	1.136
5	6.260	10.276	15.461	4.016	9.201	5.185

TABLE V
ACTUAL DISTANCE OF ARRIVAL (DOA) [m]

Placement	d1	d2	d3	d4
1	12.215	10.424	9.748	9.949
2	12.214	10.423	9.748	8.128
3	12.213	8.700	9.748	6.902
4	11.211	8.735	10.09	9.748
5	5.110	6.988	8.193	9.748

TABLE VI
ACTUAL DISTANCE DIFFERENCE OF ARRIVAL (DDOA) [m]

Placement	d12	d13	d14	d23	d24	d34
1	1.791	2.467	2.266	0.675	0.474	0.201
2	1.791	2.465	4.085	0.674	2.294	1.620
3	3.513	2.465	5.311	1.048	1.798	2.846
4	2.477	1.120	1.463	1.356	1.014	0.343
5	1.878	3.083	4.638	1.205	2.760	1.556

TABLE VII
MEASURED TIME OF ARRIVAL TOA [ns]

Placement	t1	t2	t3	t4
1	41.105	35.284	32.823	32.074
2	40.394	35.094	32.857	26.782
3	40.187	29.621	33.164	22.409
4	37.231	28.978	33.747	32.607
5	24.014	16.599	27.783	31.900

TABLE VIII
MEASURED TIME DIFFERENCE OF ARRIVAL BETWEEN THE ANTENNAS (TDOA) [ns]

Placement	t12	t13	t14	t23	t24	t34
1	5.821	8.282	9.031	2.461	3.211	0.749
2	5.300	7.538	13.612	2.238	8.312	6.075
3	10.566	7.023	17.778	3.543	7.212	10.755
4	8.253	3.484	4.624	4.769	3.628	1.140
5	7.415	3.769	7.886	11.184	15.301	4.117

TABLE IX
MEASURED DISTANCE OF ARRIVAL (DOA) [m]

Placement	d1	d2	d3	d4
1	12.332	10.585	9.847	9.694
2	12.118	10.528	9.857	8.035
3	12.056	8.886	9.949	6.723
4	11.169	8.693	10.124	9.782
5	7.204	4.980	8.335	9.570

TABLE X
MEASURED DISTANCE DIFFERENCE OF ARRIVAL BETWEEN THE ANTENNAS (DDOA) [m]

Placement	d12	d13	d14	d23	d24	d34
1	1.746	2.485	2.709	0.738	0.963	0.225
2	1.590	2.261	4.084	0.671	2.494	1.822
3	3.170	2.107	5.334	1.063	2.164	3.227
4	2.476	1.045	1.387	1.431	1.089	0.342
5	2.225	1.131	2.366	3.355	4.590	1.235

According to [1] the solution of (18) is formed by an application of the Newton–Raphson technique procedure in order to solve the nonlinear Eqs. (18):

$$F(X) = \Delta_{si} - d_{ij} = 0 \quad (18)$$

$$\Delta_{si} = \sqrt{(x_s - x_i)^2 + (y_s - y_i)^2 + (z_s - z_i)^2} \quad (19)$$

where $F(X)$ is a non-linear vector function discussed in detail by [1], $X = (x, y, z)$ is a vector variable, Δ_{si} is the distance between the arc source and the antenna i and d_{ij} is the distance difference of arc signal arrival (DDOA) between antennas i and j.

TABLE XI
ITERATION RESULTS PLACEMENT 1

Iteration	Funccount	Residual	1rst order optimality	Lambda	Norm of step
0	4	2.097	103	0.01	
1	8	1.696e-06	0.0928	0.001	0.0180604
2	12	1.569e-18	8.92e-008	0.0001	1.621e-05
3	16	6.677e-27	5.82e-012	1e-005	1.559e-11

TABLE XII
ITERATION RESULTS PLACEMENT 2

Iteration	Funccount	Residual	1rst order optimality	Lambda	Norm of step
0	4	536.336	1.55e+03	0.01	
1	8	0.134521	23.8	0.001	0.302792
2	12	9.637e-09	0.00636	0.0001	0.0049522
3	16	9.150e-23	6.2e-010	1e-005	1.326e-06

TABLE XIII
ITERATION RESULTS PLACEMENT 3

Iteration	Funccount	Residual	1rst order optimality	Lambda	Norm of step
0	4	274.046		0.01	0.235747
1	8	0.0494356		0.001	0.003254
2	12	1.797e-09		0.0001	6.21e-07
3	16	8.684e-24		1e-005	

TABLE XIV
ITERATION RESULTS PLACEMENT 4

Iteration	Funccount	Residual	1st order optimality	Lambda	Norm of step
0	4	3.0064		0.01	
1	8	3.881e-06		0.001	0.0222077
2	12	8.198e-18		0.0001	2.517e-05
3	16	2.02e-28		1e-005	3.659e-11

TABLE XV
ITERATION RESULTS PLACEMENT 5

Iteration	Funccount	Residual	1rst order optimality	Lambda	Norm of step
0	4	3204.44	2.82e+03	0.01	
1	8	13.3036	159	0.001	0.95489
2	12	0.00039818	0.858	0.0001	0.07063
3	16	3.7397e-13	2.63e-05	1e-005	0.00039
4	20	8.0779e-28	1.22e-12	1e-006	1.19e-08

TABLE XVI
ARC SOURCE POSITION [m]

Placement	Actual source			Measured source		
	x	y	z	x	y	z
1	0.0696	8.8771	5.0942	-0.133	8.1057	5.0942
2	0.0696	8.8771	5.0942	-0.048	8.4566	4.8927
3	0.0696	8.8771	5.0942	0.1185	9.0356	5.1781
4	0.0696	8.8771	5.0942	-0.073	8.4892	4.9083
5	0.0696	8.8771	5.0942	0.0715	8.7641	5.0193

TABLE XVII
ERROR IN ASCC [m]

Placement	x	y	z
1	0.2022	0.7714	0.0000
2	0.1174	0.4205	0.2015
3	0.0489	0.1585	0.0839
4	0.1425	0.3879	0.1859
5	0.0730	0.1130	0.0749

Function $F(X)$ is expanded using Taylor's series in vicinity of the root iteration $X^0 = (x^0, y^0, z^0)$ as the iteration guess point.

The non-linear system (18) was solved after 4 iterations when the sum of squared function values reaches 1.58e-25 that is less than square root of the function tolerance default set as 1.e-03, as illustrated in Table XI for the placement 1 and Tables XII, XIII, XIV and XV for placements 2, 3, 4 and 5 respectively.

Finally as illustrated Table XVI the arc source $(xyz)-$coordinates (ASCC) per placement is computed and compared with the actual ASCC as shown in Table XVII and Figs. 11, 12 and 17-18. The good performance of the proposed method in this experiment is illustrated by Fig. 11, where we can observe that the measured ASCC per placement lies inside a sphere of 1 m radius centered at the actual source coordinates namely S_o and marked with a red filled circle (○).

The measured sources are follows: S_1, S_2, S_3, S_4 and S_5 and they are respectively marked with dark blue, green, black, purple and light blue filled circle (○).In order to compare the results, we used the available actual and measured arc sources between the antennas placements shown in Table XVI.

These sources were defined by a least square iteration method as discussed above and the results are shown in Tables XI-XV.

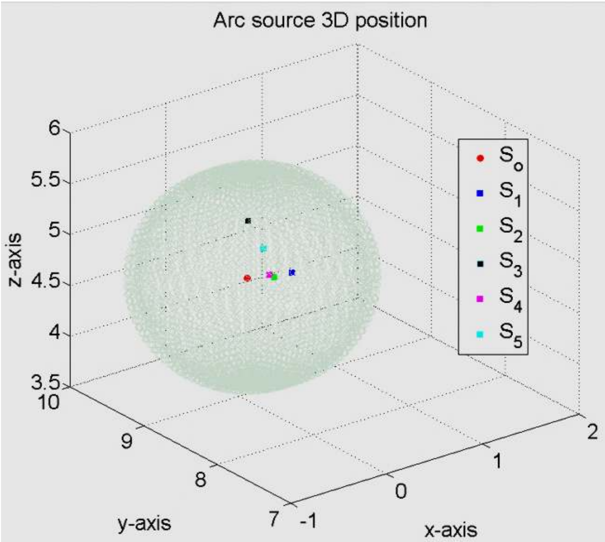

Fig. 11. Measured and actual sources observed in 3D Cartesian plane

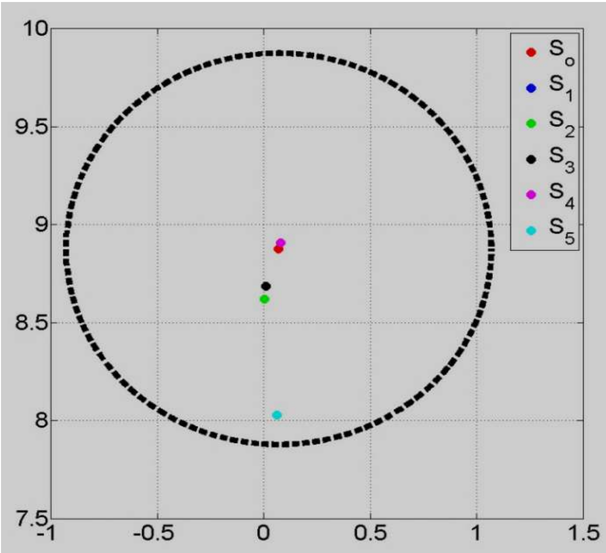

Fig. 12. Measured and actual sources observed in 2D *xy*-plane

Table XVII presents the absolute errors between the measured and estimated arc sources ASCC generated by the LSM algorithm.

We can conclude that the algorithm is suitable, since the information in the arc radiation waveforms, although corrupted measurement noise, was useful and allowed for the arc source estimation quality improvement. Figs. 12 and Figs. 17–18 show the actual and measured sources plotted in 2D Cartesian coordinates. The actual source is S_o and marked with a red filled circle (○). The measured sources are follows: S_1, S_2, S_3, S_4 and S_5 and they are respectively marked with dark blue, green, black, purple and light blue filled circle (○).

These measured sources calculated from the proposed energy method lie within a circle of 1 m radius which has its center point at the actual source 2D Cartesian coordinates. Figure 12 is the *xy*-plane when Figs. 17 and 18 are respectively *xz*- and *yz*-planes.

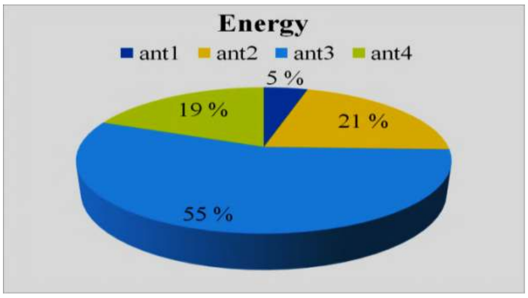

Fig. 13. Energy comparison in placement 2

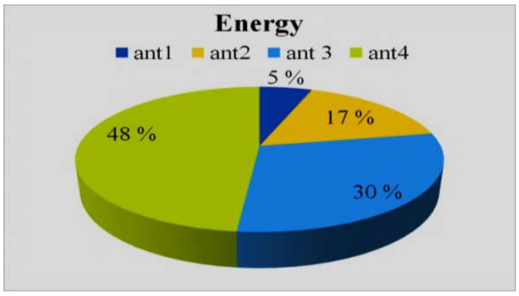

Fig. 14. Energy comparison in placement 3

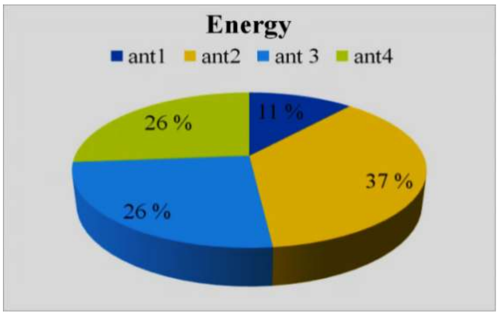

Fig. 15. Energy comparison in placement 4

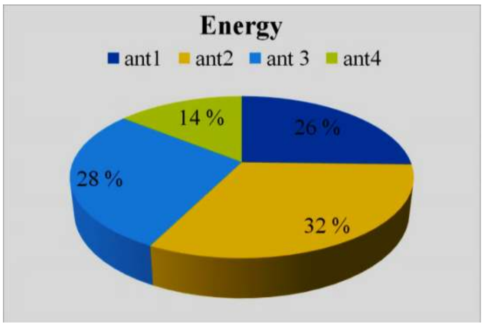

Fig. 16. Energy comparison in placement 5

IV Conclusion

This paper reported an experimental investigation of power arc source detection and location method using radio frequency signal energy measurements obtained by Yagi-Uda antennas. A new algorithm based on the signal windowing principle in order to calculate the energy adsorbed by the antennas is proposed. Such an improvement resolves the problem of arc signal time of arrival (TOA).

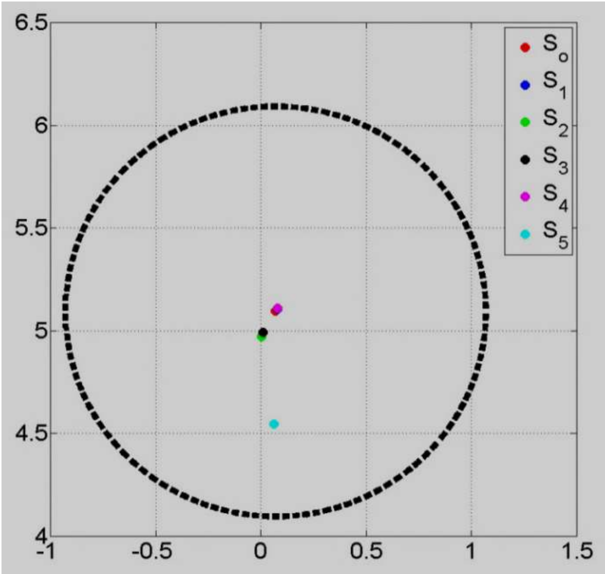

Fig. 17. Measured and actual sources observed in 2D *xz*-plane

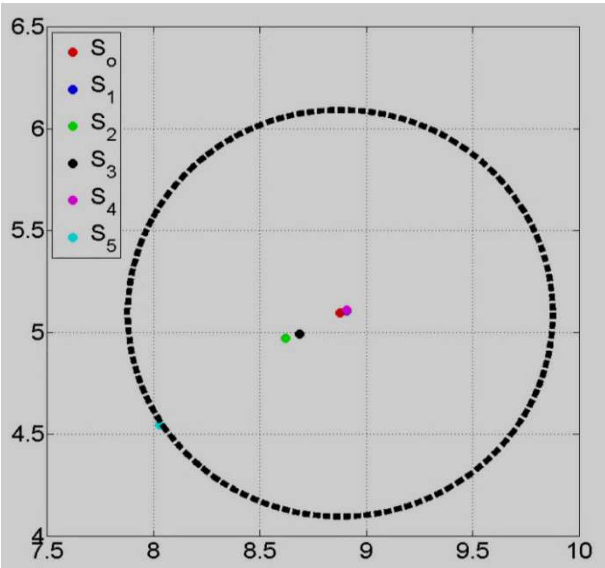

Fig. 18. Measured and actual sources observed in 2D *yz*-plan

Moreover, the problem of uncertainty of the parameters related to the external noise interferences is solved by considering only the signal FPA. This combination results in a new adaptive structure for estimating efficiently the power arcing fault source position. The results obtained through experimental data show that the proposed solution could be integrated to the distribution management system (DMS) and/or outage Management system (OMS) for accurate location of fault arcs, faster power supply restoration and minimized outage hours, in other words to enable more efficient operation under real field conditions. The convergence rate of the measured source point to the actual arc source value is acceptable. In summary, it was observed that this new proposed arcing fault detection and location method shows its potential in clarifying the location technique at a reasonable level of accuracy. Despite the good performance of this proposed method, it still has certain limitations. Since the energy absorbed by the antennas is proportional to the distance between the arc source and the receivers, it is important to define the maximum distance that allows for reliable arc location. Doing so could probably help to avoid the received signals to be buried in free space noise. It was also observed that the accuracy of this method depends on the antennas' placement. This is apparent in placement 5 where the measured ASCC presents high distance mean square error deviation when compared to the others. Furthermore obstacles such as mountains and high buildings in urban zone could also cause signals reflection, refraction and at certain point signal diffraction under raining conditions which may affect the integrity of the signal of interest and subsequently yield to measurement errors in real field conditions.

Acknowledgements

The authors gratefully acknowledge the contributions of Tatu Nieminen and Joni Klüss, for their work on building the laboratory experiment.

References

[1] Ble, F.Z., Lehtonen, M., Sihvola, A., Kim, C., Cross-correlation method for power arcing source monitoring system, (2014) *International Review of Electrical Engineering (IREE),* 9 (2), pp. 440-452.

[2] ZokoBle, F., Lehtonen, M., Kim, C., Power Arcing Source Location Using First Peak of Arrival of RF-Signal, (2014) *International Review of Electrical Engineering (IREE)*, 9 (4), pp. 873-881.

[3] Kim, C.J.; "*Electromagnetic Radiation Behavior of Low-Voltage Arcing Fault* " Power Delivery, IEEE Transactions on Vol. 24 , 2009 , Pp: 416 - 423

[4] Bartlett, E.J.; Moore, P.J.; "*Remote sensing of power system arcing faults"*, Advances in Power System Control, Operation and Management, 2000. APSCOM-00. 2000 International Conference on Vol. 1 , 2000, pp. 49–53

[5] Moore, P.J.; Portugues, I.E.; Glover, I.A.; "*Radiometric location of partial discharge sources on energized high-Voltage plant"*, Power Delivery, IEEE Transactions on Vol. 20, 2005, pp. 2264-2272

[6] Shihab, S.; Wong, K.L.; *"Detection of faulty components on power lines using radio frequency signatures and signal processing techniques"*, Power Engineering Society Winter Meeting, 2000. IEEE Vol. 4, 2000, pp. 2449–2452

[7] Young, D.P.; Keller, C.M.; Bliss, D.W.; Forsythe, K.W.*; "Ultra-wideband (UWB) transmitter location using time difference of arrival (TDOA) techniques"*, Signals, Systems and Computers, 2003. Conference Record of the Thirty-Seventh Asilomar Conference on Vol. 2 , 2003, pp. 1225–1229

[8] Sun, Y.; Stewart, B.G.; Kemp, I.J.*; "Alternative cross-correlation techniques for location estimation of PD from RF signal"*, Universities Power Engineering Conference, 2004. UPEC 2004. 39th International Vol. 1, 2004, pp. 143–148

[9] Chye Huat Peck; Moore, P.J.; *"A direction-finding technique for wide-band impulsive noise source"*, Electromagnetic Compatibility, IEEE Transactions on Vol. 43, 2001, pp. 149–1544

[10] Yang, L.; Judd, M.D.; Bennoch, C.J.*; "Time delay estimation for UHF signals in PD location of transformers [power transformers]"*, Electrical Insulation and Dielectric Phenomena, 2004. CEIDP '04. 2004 Annual Report Conference, 2004, pp. 414-417

[11] Azaria, M.; Hertz, D.; *"IEEE Transactions on Acoustics, Speech, and Signal Processing"*, Vol. 32, 1984, pp. 280-285

[12] Soeta, Y.; Uetani, S.; Ando, Y.; *"Autocorrelation and cross-correlation analyses of alpha waves in relation to subjective preference of a flickering light"*, Engineering in Medicine and Biology Society, 2001. Proceedings of the 23rd Annual International Conference of the IEEE Vol. 1, 2001, pp. 635– 638

[13] Alavi, B.; Pahlavan, K.; *"Modeling of the TOA-based distance measurement error using UWB indoor radio measurements"*, Communications Letters, IEEE Vol. 10, 2006, pp. 275–277

[14] Mallat, Achraf; Louveaux, J.; Vandendorpe, L.; *"UWB based positioning: Cramer Rao bound for Angle of Arrival and comparison with Time of Arrival"*, 2006 Symposium on Communications and Vehicular Technology, pp. 65–68

[15] Alsindi, N.; Xinrong Li; Pahlavan, K.; *"Analysis of Time of Arrival Estimation Using Wideband Measurements of Indoor Radio Propagations"*,Instrumentation and Measurement, IEEE Transactions on Vol. 56, 2007, pp. 1537-1545

[16] Rohrig, C.,Kunemund, F., *"Mobile Robot Localization using WLAN Signal Strengths"*.Intelligent Data Acquisition and Advanced Computing Systems: Technology and Applications, 2007. IDAACS 2007. 4th IEEE Workshop, pp. 704 - 709

[17] Bo-ChiehLiu,Ken-Huang Lin *"Accuracy Improvement of SSSD Circular Positioning in Cellular Networks"*.Vehicular Technology, IEEE Transaction, pp. 1766 - 1774

[18] Motter, P. , Allgayer, R.S. ; Muller, I. ; Pereira, C.E. ; Pignaton de Freitas, E. *"Practical issues in Wireless Sensor Network localization systems using received signal strength indication"*.Sensors Applications Symposium (SAS), 2011 IEEE, pp. 227 - 232

[19] Chih-Chun Lin, She-Shang Xue; Yao, L. *"Position Calculating and Path Tracking of Three Dimensional Location System Based on Different Wave Velocities"*.Dependable, Autonomic and Secure Computing, 2009. DASC '09. Eighth IEEE International Conference, pp. 436 - 441

[20] El Arja, H., Huyart, B.; Begaud, X. *"Joint TOA/DOA measurements for UWB indoor propagation channel using MUSIC algorithm"*.Wireless Technology Conference, 2009, pp. 124 - 127

[21] Born, A.,Schwiede, M. ; Bill, R. *"On distance estimation based on radio propagation models and outlier detection for indoor localization in Wireless GeosensorNetworks"*,Indoor Positioning and Indoor Navigation (IPIN), International Conference 2010, pp. 1 - 6

[22] Fugen Su, WeizhengRen; Hongli Jin, *"Localization Algorithm Based on Difference Estimation for Wireless Sensor Networks"*.Communication Software and Networks. ICCSN '09. International Conference, 2009, pp. 499 - 503

[23] Bing-Fei Wu , Cheng-Lung Jen ; Kuei-Chung Chang, *"Neural fuzzy based indoor localization by Kalman filtering with propagation channel modeling"*. Systems, Man and Cybernetics. ISIC. IEEE International Conference, 2007, pp. 812 - 817

[24] Benkic, K., Malajner, M.; Planinsic, P.; Cucej, Z. *"Using RSSI value for distance estimation in wireless sensor networks based on ZigBee"*.Systems, Signals and Image Processing, 2008. 15th International Conference, 2008, pp. 303 - 306

[25] Suk-Un Yoon, Liang Cheng; Ghazanfari, E.; Pamukcu, S.; Suleiman, M.T. *"A Radio Propagation Model for Wireless Underground Sensor Networks"*.Global Telecommunications Conference (GLOBECOM 2011), 2011, pp. 1 – 5

[26] Fengzhen Wang; Lo, T.; Litva, J.; Reed, W.; "*High accuracy direction finding antenna array system*" Antennas and Propagation Society International Symposium, 1994. AP-S. Digest 1994 Vol..3, pp: 1544 - 1547

[27] Portugues, I.; Moore, P.J.; Glover, I.A.; "*Frequency domain characterisation of partial discharges via a non-invasive measurement system*" Properties and Applications of Dielectric Materials, 2003. Proceedings of the 7th International Conference on 2003 Vol.3, pp: 835 - 838

[28] Moore, P.; Crossley, P.; "*GPS applications in power systems, Part. I. Introduction to GPS*" Power Engineering Journal Vol. 13 , 1999 , pp: 33 - 39

[29] Judd, M.D.; Li Yang; Hunter, I.B.B. "*Partial discharge monitoring of power transformers using UHF sensors. Part I: sensors and signal interpretation*"; Electrical Insulation Magazine, IEEE Vol. 21 , 2005 , pp: 5 - 14

[30] Moore, P.J.; Bartlett, E.J.; Vaughan, M.; "*Fault location using radio frequency emissions*" Developments in Power System Protection, 2001, Seventh International Conference on (IEE) 2001 , pp: 331 – 334

[31] Chin-Lung Yang; Bagchi, S.; Chappell, W.J.; " *Location tracking with directional antennas*" in wireless sensor networks Microwave Symposium Digest, 2005 IEEE MTT-S International 2005

[32] Li Cong; Weihua Zhuang; "*Hybrid TDOA/AOA mobile user location for wideband CDMA cellular systems Wireless Communications*", IEEE Transactions Vol. 1 , 2002 , pp: 439 – 447

[33] Babnik, T.; Aggarwal, R.K.; Moore, P.J.; Wang, Z.D.; " *Radio frequency measurement of different discharges*" Power Tech Conference Proceedings, 2003 IEEE Bologna Vol. 3 2003

[34] Afef Ben Hadj Alaya-Feki; Moulines, E.; Villebrun, E.; "*Exploiting Radio Measurements in Wireless Mobile Networks with Advanced Signal Processing*" Wireless and Mobile Communications, 2007. ICWMC '07. Third International Conference on 2007 , pp: 28 – 28

[35] Portugues, I.E.; Moore, P.J.; " *Study of propagation effects of wideband radiated RF signals from PD activity*" Power Engineering Society General Meeting, 2006. IEEE 2006

[36] Alavi, B.; Pahlavan, K.; "*Modeling of the TOA-based distance measurement error using UWB indoor radio measurements*" Communications Letters, IEEE Vol. 10 , 2006 , pp: 275 – 277

[37] Damazio, D.O.; Takai, H.; "*A radio detector system for ultra high energy cosmic showers* "Nuclear Science Symposium Conference Record, 2003 IEEE Vol. 1 2003 , pp: 134 - 138

[38] Damazio, D.O.; Takai, H.; "*The cosmic ray radio detector data acquisition system*" Nuclear Science Symposium Conference Record, 2004 IEEE Vol. 2 2004 , pp: 1205 - 1211

[39] Gang Zhou; Haiyun Tang; Lau, K.Y.; "*In-building radio distribution using a "saturated" distributed-antenna-architecture-universal radio-power and delay-spread statistics*" Communications, 1999. ICC '99. 1999 IEEE International Conference on Vol. 1 1999 , pp: 29 - 35

[40] Joyce, R.M.; Barker, D.E.; McCarthy, M.A.; Feeney, M.T.; "*A study into the use of polarisation diversity in a dual band 900/1800 MHz GSM network in urban and suburban environments*" Antennas and Propagation, 1999. IEE National Conference on.1999 , pp: 316 – 319

[41] Moore, P.J.; "*Radiometric measurement of Circuit Breaker interpole switching times*" Power Delivery, IEEE Transactions on Vol. 19 , 2004 , pp: 987 – 992

[42] Shih-Hau Fang; Jen-Chian Chen; Hau-Ru Huang; Tsung-Nan Lin; "*Metropolitan-Scale Location Estimation Using FM Radio with Analysis of Measurements*" Wireless Communications and Mobile Computing Conference, 2008. IWCMC '08. International 2008 , pp: 171 – 176

[43] Aragon-Zavala, A.; Belloul, B.; Nikolopoulos, V.; Saunders, S.R.; "*Accuracy evaluation analysis for indoor measurement-based radio-wave-propagation predictions*" Microwaves, Antennas and Propagation, IEE Proceedings - Vol. 153 , 2006 , pp: 67 – 74

[44] Chiang, R.I.C.; Rowe, G.B.; Sowerby, K.W.; "*A Quantitative Analysis of Spectral Occupancy Measurements for Cognitive Radio*" Vehicular Technology Conference, 2007. VTC2007-Spring. IEEE 65th 2007

[45] Karttunen, P.; Kalliola, K.; Laakso, T.; Vainikainen, P.; "*Measurement analysis of spatial and temporal correlation in wideband radio channels with adaptive antenna array*" Universal Personal Communications, 1998. ICUPC '98. IEEE 1998 International Conference on Vol. 1 1998 , pp: 671 - 675

[46] Kaindl, A.; Nowak, S.; Koschnitzki, T.; Borsi, H.; "*Practical application of partial discharge measurements at epoxy impregnated coils for analyzing signal noise in the radio frequency range*" Electrical Insulation, 2000. Conference Record of the 2000 IEEE International Symposium on 10.1109/ELINSL.2000.845481 2000 , pp: 168 - 171

[47] Saadane, R.; Khafaji, A.; Wahbi, M.; El Bhiri, B.; Aboutajdine, D.; "*Ultra wide bandwidth radio channel indoor propagation and path loss analysis based on measurements*" Multimedia

Computing and Systems, 2009. ICMCS '09. International Conference on 2009 , pp: 259 – 263

[48] Rafferty, W.; Anderson, J.; Saulnier, G.; Holm, J.; "*Laboratory Measurements and a Theoretical Analysis of the TCT Fading Channel Radio System*" Communications, IEEE Transactions on Vol. 35 , 1987 , pp: 172 – 180

[49] Soldanels, Roy M.; "*Flexible Radio Frequency Bonding Configurations: Theoretical Analysis, Measurements, and Practical Applications*" Electromagnetic Compatibility, IEEE Transactions on Vol. 9 , 1967 , pp: 136 – 138

[50] Santella, G.; Restuccia, E.; "*Analysis of frequency domain wide-band measurements of the indoor radio channel at 1, 5.5, 10 and 18 GHz*" Global Telecommunications Conference, 1996. GLOBECOM '96. 'Communications: The Key to Global Prosperity Vol. 2 1996 , pp: 1162 - 1166

[51] Shaw, V.L.; Berchi, F.G.; McRue, W.H.; "*Auto And Cross Correlation Analysis Of Environment, System And Target Parameters For Iceberg Detection Using Airborne Radar*" Geoscience and Remote Sensing Symposium, 1988. IGARSS '88. Remote Sensing: Moving Toward the 21st Century., International Vol. 2 1988 , pp: 809 - 816

[52] Elkalashy, N.I., Lehtonen, M. ; Darwish, H.A. ; Izzularab, M.A. ; Taalab, A.-M.I. "*Modeling and experimental verification of high impedance arcing fault in medium voltage networks*" Dielectrics and Electrical Insulation, IEEE Transactions on Vol.14 , 2007,pp: 375 - 383

Authors' information

Frank Zoko Ble obtained a B.Sc. in Physics in Ivory coast National University, Abidjan in 1997. He received M.Sc. in Electrical Engineering in Helsinki University of Technology (TKK), Espoo, Finland in 2010. He is a planning and design engineer for the City of Espoo, the central municipality enterprise, Finland. Also, he is working toward his PhD degree in Aalto University, School of Electrical Engineering. His research interests are in electric power arcs detection using radio frequency measurements. He is a researcher in the Department of Electrical Engineering and Automation of Aalto University, School of Electrical Engineering, Finland.

Matti Lehtonen (1959) was with VTT Energy, Espoo, Finland from 19987 to 2003, and since 1999 has been a professor at the Helsinki University of Technology (TKK), where he is now head of Electrical Engineering department. MattiLehtonen received both his Master's and Licentiate degrees in Electrical Engineering from Helsinki University of Technology , in 1984 and 1989 respectively, and the Doctor of Technology degree from Tampere University of technology in 1992. The main activities of Professor Lehtonen include power system planning and asset management, power system protection including earth fault problems, harmonic related issues and applications of information technology in distribution systems. He is a Professor in Aalto University, School of Electrical Engineering, Finland.

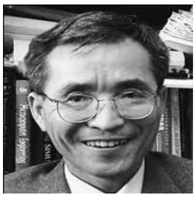

Charles Kim received a PhD degree in electrical engineering from Texas A&M University (College Station, TX) in 1989. Since 1999, he has been with the Department of Electrical and Computer Engineering at Howard University. Previously, Dr. Kim held teaching and research positions at Texas A&M University and the University of Suwon. Dr. Kim's research includes failure detection, anticipation, and system safety analysis in safety critical systems in energy, aerospace, and nuclear industries. Several inventions of his in the research area have been patent field through the university's intellectual property office. Dr. Kim is a senior member of IEEE and the chair of an IEEE chapter in Washington Baltimore section.